Modelling of a 4 Axis Parallel Machine for Heavy Parts Handling

Olivier Company, Sébastien Krut, François Pierrot

Modelling of a 4-Axis Parallel Machine for Heavy Parts Handling

Company, O.; Krut, S.; Pierrot, F.

Abstract

This paper presents a new 4-degree-of-freedom parallel mechanism dedicated to handling of heavy parts within a large workspace. These 4 degrees of freedom are 3 translations and 1 rotation about a given axis. Such a mechanism is rare; most of common parallel mechanisms have 3 or 6 degrees of freedom. Firstly, a description of the mechanism is given. Then models are derived regarding velocity and force transformation as input-output relationships. Finally, internal forces models and stiffness model are evaluated. All models are embedded in a software module aiming to help with preliminary design of machines based on this new architecture.

1 Notation

$\mathbf{I_3}$	identity matrix of rank 3
pre(*X*)	pre-cross-product matrix associated to vector *X*
P_i	point P_i
$\boldsymbol{P}_i$	vector containing Cartesian coordinates of point P_i
P	matrix containing Cartesian coordinates of all points P_i

1 Introduction

Recently, a fast machine-tool based on Delta concept, Urane Sx [**1**], has been built and its performances are a *3.5g* guaranteed acceleration on the whole workspace (with up *to 5.0g* for a sub part of the workspace). So, parallel mechanisms are a good choice to achieve very fast operations, and both machining and robotics fields already appreciated their efficiency. This paper attends to show that parallel mechanisms could also be used to build fast **handling** machines where until nowadays only gantry-like devices are used. The case study presented in this paper regards handling machines for heavy parts (more than *100 kg*) such that parts handled in automotive and truck industry: crankshafts, flywheels, cylinder heads, etc.

For the considered application – handling of heavy parts – 4 degrees of freedom are needed: three translations to move the part from point to point, one rotation (often about a vertical axis) to orient it. In some regards, this can be seen as very similar to pick-and-place; however two key characteristics of handling applications are really specific: (i) parts are heavier than in pick-and-place applications (more than *100 kg*, compared to a typical *1 kg* object), (ii) the workspace is larger and often has one dimension that is dramatically different from the others. For example, in this paper, numerical studies will concern *116 kg* parts and a *3.0mx0.5mx0.5m* workspace (with a complete rotation about the vertical axis).

Most of existing parallel mechanisms and robots have 3 or 6 degrees of freedom. Only very few have 4 degrees of freedom [**2**] [**3**] [**4**] [**5**] [**6**], and none of them offer the 3-translation, 1-rotation combination needed for handling. Even the Delta with its additional, non-parallel, fourth degree of freedom cannot fulfil the requirements: it is not possible to add such a telescopic passive chain for a several-meter long workspace. The aim of this paper is to present a mechanism that provides the needed 4 degrees of freedom (3 translations and 1 rotation about a given axis) and then to study it in details. After a short description of its mechanical architecture, geometry and kinematics modelling are presented. Then forces transmission between actuators and nacelle as well as internal forces models are derived. A simplified stiffness analysis and an accuracy study are also carried out. To offer numerical examples, a software module has been developed to embed all these models. It allows to very quickly and very easily select most machine components key dimensions.

2 The mechanism

A CAD drawing of the considered mechanism is presented in Fig. 1, and Fig. 2 is a "Joints and Loops Graph" showing the different joints (Each box stands for a joint; S: spherical, R: revolute, P: prismatic), pointing out the actuated joints (A grey box means that the joint is actuated) and describing the way the kinematic loops are arranged. One can immediately note that the mechanism has 8 internal degrees of freedom: each link connected to neighbours by two S joints can rotate about the axis passing by the S joints centres. If needed for technological reasons, this can be suppressed by replacing one of the S joint by a Universal joint – U Joint – ; the mechanism would then become isostatic; moreover, if hyperstatic construction is made possible by very accurate machining and assembly (or by accepting local deformations) it is even feasible to replace all S joints by U joints.

In Fig. 3a scheme, it can be seen that the proposed mechanism belongs to the Delta-Hexa "family": actuators are fixed on the base, and links of constant length are connected to the nacelle. The main interest of using spatial parallelograms lies in the fact that the bars are only stressed in tension-compression (see **[7]** for a less stiff parallel mechanism using one bar and universal joints instead of spatial parallelograms). This kind of stress is easier to manage than torsion and flexion and the consequences are a good stiffness of the whole machine.

Fig. 1: *Machine presentation*

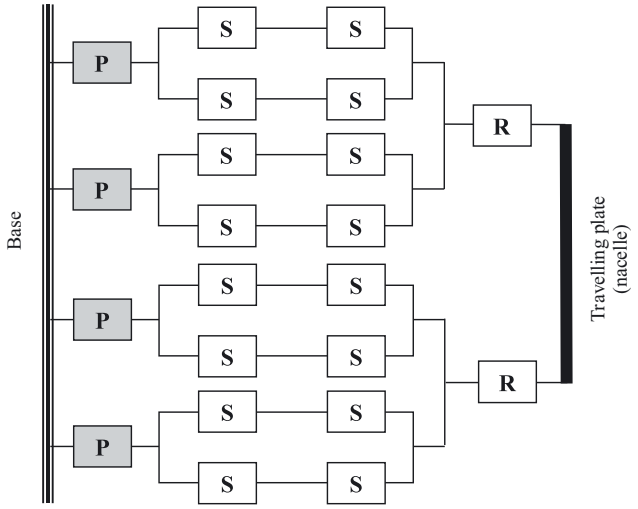

Fig. 2.: *Joints and Loops Graph*

The machine uses "pairs" of rods linking each motor to the nacelle; the key issue in designing this four-degree-of-freedom machine is to build a non-rigid nacelle to obtain the additional rotation. The shape of the articulated travelling plate looks like letter "H" where two revolute joints are located on each end of the central bar. The two lateral bars have the same behaviour as if they belong to a Delta-like robot that is to say that their possible displacements are only translations. A displacement of one lateral bar of the "H" relative to the other one produces the desired rotation about **z** axis.

Here, 4 linear actuators are used; they are parallel to the longest displacement direction, so the machine is well suited to workspace specifications.

The denomination of points used in following models is introduced in Fig. 3b. The mechanism description is as follows:

– P_i is the origin of prismatic joint *i* belonging to chain *i*

– $\boldsymbol{U_i}$ is the unit vector giving the direction of the prismatic joint

– q_i is the position of actuator number *i*. q_i is counted positive in the direction of $\boldsymbol{U_i}$

– A_{i1} and A_{i2} are the joints centres (spherical or universal) at actuators side

– A_i is the middle of $[A_{i1}\ A_{i2}]$

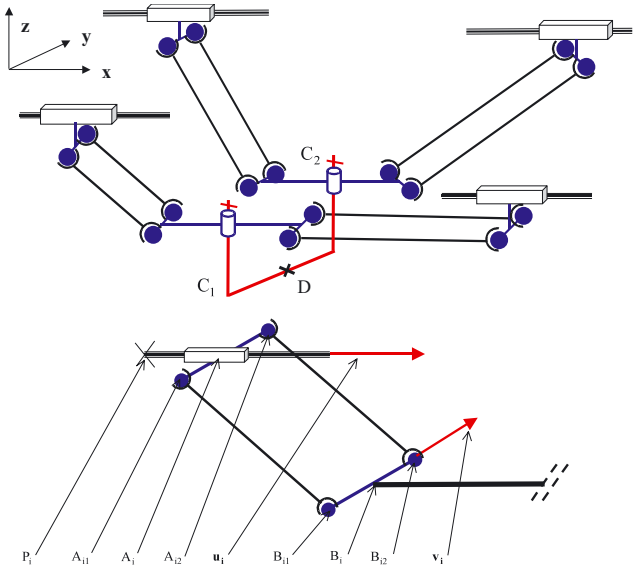

Fig. 3: *Description for modelling*

– B_{i1} and B_{i2} are the joints centre (spherical or universal) at nacelle side

– B_i is the center of $[B_{i1}\ B_{i2}]$

– V_i is the unit vector whose direction is given by $A_{i1}\ A_{i2}$ (or $B_{i1}\ B_{i2}$)

– d_i is equal to half the distance between A_{i1} and A_{i2} (or B_{i1} and B_{i2})

– L_i is the length of chain i rods (the rods in a given pair are supposed to have the same length)

– the union of chains 1 and 2 (respectively 3 and 4) is called "metachain 1" (respectively "metachain 2")

– the direction of revolute joints at points C_1 and C_2 is given by vector ***W***

– the end point of the mechanism is point D

– The centre of mass of the carried object is point E.

If some geometric constraints are satisfied [**8**], the 4 degrees of freedom of the end part are three translations and one rotation about a given axis. For the presented mechanism, these constraints are:

– the bars in a pair must remain parallel and have the same length,
– the chosen geometry is not always singular (For example, if all vectors $\boldsymbol{V_i}$ are parallel, the mechanism is always singular and gets one uncontrolled degree of freedom).

3 Position relationships

The relation between the actuators position $\left(\boldsymbol{Q} = \left[q_1 \quad \cdots \quad q_4\right]^T\right)$ and the nacelle position (X expressed in the fixed reference frame) is derived in this section. X is expressed as $\boldsymbol{X} = \left[\boldsymbol{x^T} \quad \theta\right]^T$, where x is the vector composed by the Cartesian coordinates of point D in the reference frame, and θ is the angle describing the rotation of C1C2 about $\boldsymbol{W}$.

Inverse model

Only the relation giving Q as a function of X can always be computed in an analytical way whatever the mechanism arrangement is. Indeed, given X, for chain number i, a second order polynomial expression is obtained:

$$q_i^2 - 2(\boldsymbol{B_i} - \boldsymbol{P_i}) \cdot \boldsymbol{U_i} q_i + (\boldsymbol{B_i} - \boldsymbol{P_i})^2 - L_i^2 = 0 \tag{1}$$

If the pose of the nacelle is reachable, this polynomial has 2 real roots. According to the choice of counting q_i positive in the direction of vectors $\boldsymbol{U_i}$, only the largest root of the polynomial is considered because it corresponds to the proper configuration of the mechanism.

Direct model

For some particular arrangements (for example the one presented in Fig. 1), $\boldsymbol{X}$ as a function of $\boldsymbol{Q}$ can be expressed in closed form. In that case, geometrical parameters are:

$$\mathbf{P} = \begin{bmatrix} 0 & 0 & 0 & 0 \\ -p & -p & p & p \\ 0 & 0 & 0 & 0 \end{bmatrix} \quad \mathbf{U} = \begin{bmatrix} -1 & 1 & 1 & -1 \\ 0 & 0 & 0 & 0 \\ 0 & 0 & 0 & 0 \end{bmatrix} \quad (\mathbf{DC})_0 = \begin{bmatrix} 0 & 0 \\ -d & d \\ 0 & 0 \end{bmatrix}$$

$$\mathbf{CB} = \begin{bmatrix} -d & d & d & -d \\ 0 & 0 & 0 & 0 \\ 0 & 0 & 0 & 0 \end{bmatrix}$$

$$\boldsymbol{L} = L\begin{bmatrix} 1 & 1 & 1 & 1 \end{bmatrix} \qquad \boldsymbol{W} = \begin{bmatrix} 0 & 0 & 1 \end{bmatrix}$$

With such data, position equations can be written as follows:

$$\begin{cases} (x + d\sin\theta - d + q_1)^2 + (y - d\cos\theta + p)^2 + z^2 = L^2 \\ (x + d\sin\theta + d - q_2)^2 + (y - d\cos\theta + p)^2 + z^2 = L^2 \\ (x - d\sin\theta + d + q_3)^2 + (y + d\cos\theta - p)^2 + z^2 = L^2 \\ (x - d\sin\theta - d + q_4)^2 + (y + d\cos\theta - p)^2 + z^2 = L^2 \end{cases} \tag{2}$$

Manipulating equations leads to:

$$\begin{cases} (x + d\sin\theta - d + q_1)^2 + (y - d\cos\theta + p)^2 + z^2 = L^2 \\ (2d - q_2 - q_1)(2x + 2d\sin\theta - q_2 + q_1) = 0 \\ (2d - q_3 + q_4)(2x - 2d\sin\theta - q_3 + q_4) = 0 \\ (2d\sin\theta + 2d - q_1 - q_3)(2x + q_1 - q_3) + 2y(2d\cos\theta - 2p) = 0 \end{cases} \tag{3}$$

Finally, direct geometry model is obtained for this particular arrangement:

$$\begin{cases} z = \pm\sqrt{L^2 - (x + d\sin\theta - d + q_1)^2 - (y - d\cos\theta + p)^2} \\ y = -\dfrac{(2d\sin\theta + 2d - q_1 - q_3)(2x + q_1 - q_3)}{2d\cos\theta - 2p} \\ x = \dfrac{-q_1 + q_2 + q_3 - q_4}{4} \\ \theta = Arc\sin\left(\dfrac{-q_1 + q_2 - q_3 + q_4}{4d}\right) \end{cases} \tag{4}$$

4 Kinematics analysis and workspace evaluation

Kinematics analysis (ie. velocity transformation) and workspace evaluation are closely related issues; as a matter of fact, there is a dramatic difference between "reachable" workspace, and "usable" workspace, and this difference can be taken into account thanks to kinematics relationship. Indeed, if a "reachable" location is a location where polynomial (D) has 2 real roots, a "usable" location is a "reachable" location where the machine will work properly with respect to accuracy-based or stiffness-based criteria. Such issues can be addressed at a preliminary stage by resorting to some properties of the velocity relationship.

Reachable workspace

A simple flooding technique is used to find the reachable workspace. For this method, a starting point belonging to the workspace is needed. Then, a sphere (initially of unit radius) is expanded towards reaching the workspace boundaries with a given precision. Plot of Fig. 4a is obtained for the selected mechanism (see appendix for numerical values of its dimensions).

Well conditioned workspace

In the Fig. 6b plot, all the positions are reachable in a theoretical way, but practically some of them are singular or cannot be reached physically due to collisions between bars and actuators for example. So a "safe" subset of the reachable workspace must be selected. Jacobian matrix *J* is used in the relation between actuators velocity $\dot{\boldsymbol{Q}}$ and nacelle velocity in the cartesian space $\dot{\boldsymbol{X}}$. This relation can be written as follows:

$$\dot{\boldsymbol{X}} = \mathbf{J}\dot{\boldsymbol{Q}} \tag{5}$$

For serial robots, the elements of matrix **J** are finite numbers because they depend on robot physical dimensions. The problem with parallel mechanisms is that the relation (**5**) comes from the following relation:

$$\mathbf{J}_x\dot{\boldsymbol{X}} = \mathbf{J}_q\dot{\boldsymbol{Q}} \tag{6}$$

In relation (18) $\mathbf{J}_x$ and $\mathbf{J}_q$ elements are finite numbers depending on physical dimensions of the machine, but both matrices can become singular. So minimum or maximum singular values, or determinant of **J** are not good criteria as their values can be *either* zero *or* infinite in a singular point. For hexapod-like machines kinematics can be written according to

equation (**6**) where $\mathbf{J_q} = \mathbf{I_n}$. So, according to equations (5) and (6), **J** can be written as $\mathbf{J} = \mathbf{J_x^{-1}}\,\mathbf{I_n}$. If **J** is singular, it is due to the fact that $\mathbf{J_x}$ is also singular: $\sigma_{\mathbf{max}}(\mathbf{J}) = +\infty \Leftrightarrow \sigma_{\mathbf{max}}\left(\mathbf{J_x^{-1}}\right) = +\infty \Leftrightarrow \sigma_{\mathbf{max}}(\mathbf{J_x}) = 0$. As singular values of $\mathbf{J_x}$ are always finite numbers, for an hexapod-like machine, when **J** is singular, the machine gains degrees of freedom that is to say stiffness vanishes. For parallel machines having fixed actuators, both $\mathbf{J_x}$ and $\mathbf{J_q}$ can have a singular value equal to zero. For such machines, **J** can be expressed as $\mathbf{J} = \mathbf{J_x^{-1}}\,\mathbf{J_q}$. So both types of singularities can occur that is to say the machine can gain or loose degrees of freedom. In that case, the jacobian condition number is a good measuring index [**9**] because a singular position corresponds to $\sigma_{\mathbf{min}}(\mathbf{J_x}) = 0$ or $\sigma_{\mathbf{min}}\left(\mathbf{J_x^{-1}}\right) = +\infty \Leftrightarrow \sigma_{\mathbf{max}}(\mathbf{J_x}) = 0$ and by consequence $cond(\mathbf{J}) = \dfrac{\sigma_{\mathbf{max}}(\mathbf{J})}{\sigma_{\mathbf{min}}(\mathbf{J})} = +\infty$. To establish equation (6), the classical property that relates the velocities, ***V****(A)* and ***V****(B)* of two points A and B belonging to the same rigid body is used:

$$\boldsymbol{V}(B) \cdot \boldsymbol{AB} = \boldsymbol{V}(B) \cdot \boldsymbol{AB} \tag{7}$$

Applying this relation to the four chains leads to:

$$\mathbf{J_x} = \left[\boldsymbol{A_iB_i}^{T} \quad \boldsymbol{(DC_j \times A_iB_i).W}\right] \tag{8}$$

and:

$$\mathbf{Jq} = \mathbf{diag}\ (\boldsymbol{A_iB_i}\,.\boldsymbol{V_i}) \tag{9}$$

The method used to compute the "usable" workspace (that is to say well conditioned workspace) is to only keep the points that guarantee a minimal value of the selected criteria. To do that, the minimal value of the condition number on the whole reachable workspace is searched by optimisation. Then a safety coefficient is chosen: only the points where the condition number is smaller than the product of the minimal condition number by the selected coefficient are kept.

Regarding self-collisions, for the given range of variation for θ (that is to say +/–45°), it is not useful to study the problem of self collisions: if the nacelle design respects some simple rules, the bars will never collide using well conditioned workspace. An example of this workspace is plotted in Fig 4b. On this plot, well conditioned workspace is more than two times smaller than the reachable workspace: this shows the importance of such a computation.

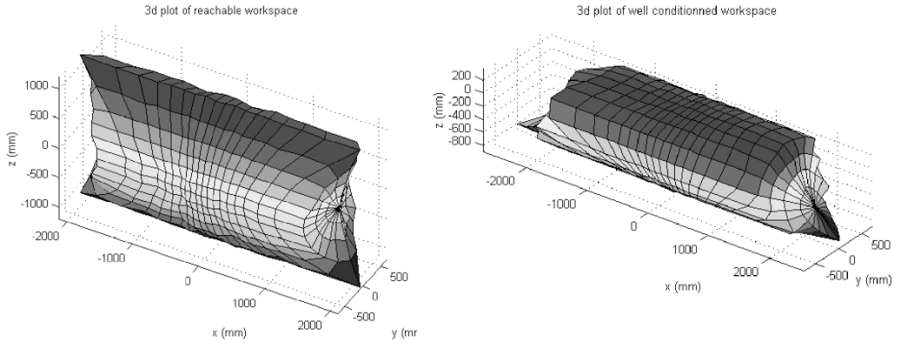

Fig. 4: *3D plot of workspace.*

5 Statics analysis

To design the mechanism, maximal forces have to be known: actuators forces are needed to select them, and internal forces are needed to design joints and others machine components.

Actuator forces

For a nacelle given pose and a given force, $\boldsymbol{F_{ext}}$, and torque, $\boldsymbol{M_{ext}}$, applied on it, the resulting force on the actuators $\boldsymbol{F_{mot}}$ is given by:

$$\boldsymbol{F_{mot}} = \begin{bmatrix} \boldsymbol{F_{ext}} \\ \boldsymbol{M_{ext}} \cdot \boldsymbol{Z} \end{bmatrix} \tag{10}$$

A plot of maximal forces on the actuators is given in Fig 5a. This plot shows that the selected geometry and dimensions are not optimal because forces in actuators vary by a factor of four: the behaviour of the machine is far from being constant in the workspace.

Bar forces

The forces in bars are another important point for dimensioning machine components. Given that value and the desired load, convenient size and material can be found. This load is also useful to size passive joints. Until now, for geometry and kinematics modelling, each spatial parallelogram was considered as a single bar. For the computation of forces in bars, bars in a spatial parallelogram must be distinguished. Each bar has ball joints at its ends, so the stress in each bar is only tension or compression along its axis (*ie* A_iB_i)

Nacelle's balance can be written as follows:

$$\begin{cases} \sum_{i=1}^{4}\sum_{j=1}^{2} f_{ij}\,\dfrac{\boldsymbol{A_{ij}}\,\boldsymbol{B_{ij}}}{L_{ij}} = \boldsymbol{F_{ext}} \\ \sum_{i=1}^{4}\sum_{j=1}^{2} f_{ij}\,\dfrac{\boldsymbol{A_{ij}}\,\boldsymbol{B_{ij}}}{L_{ij}} \times \boldsymbol{B_{ij}E} = \boldsymbol{M_{ext}} \\ \sum_{i=1}^{2}\sum_{j=1}^{2}\left(f_{ij}\,\dfrac{\boldsymbol{A_{ij}}\,\boldsymbol{B_{ij}}}{L_{ij}} \times \boldsymbol{B_{ij}C_1}\right)\cdot \boldsymbol{W} = 0 \\ \sum_{i=3}^{4}\sum_{j=1}^{2}\left(f_{ij}\,\dfrac{\boldsymbol{A_{ij}}\,\boldsymbol{B_{ij}}}{L_{ij}} \times \boldsymbol{B_{ij}C_2}\right)\cdot \boldsymbol{W} = 0 \end{cases} \tag{11}$$

where:

– i stands for chain number i (see Fig. 3), j stands for the bar number j in the considered chain

– f_{ij} is the algebraic value of the stress in the considered bar

– $\boldsymbol{F_{ext}}$ and $\boldsymbol{M_{ext}}$ are vectors of external force and moment acting at point E

This system is composed of 8 algebraic equations:

– are related to forces

– 3 are related to torques

– 2 equations representing the fact that there is no torque around the nacelle revolute joints axis.

System of equations (11) can be written in a linear form as follows, assuming that all the bars have the same length *L*:

$$\mathbf{J_b} = \frac{1}{L}\begin{bmatrix} \boldsymbol{AB_{11}} & \boldsymbol{AB_{12}} & \dots & \boldsymbol{AB_{12}} \\ \boldsymbol{AB_{11}} \times \boldsymbol{B_{11}E} & \boldsymbol{AB_{12}} \times \boldsymbol{B_{21}E} & \dots & \boldsymbol{AB_{42}} \times \boldsymbol{B_{42}E} \\ (\boldsymbol{AB_{11}} \times \boldsymbol{B_{11}C_1}) \cdot \boldsymbol{W} & (\boldsymbol{AB_{12}} \times \boldsymbol{B_{12}C_1}) \cdot \boldsymbol{W} & \dots & \boldsymbol{0} \\ \boldsymbol{0} & \boldsymbol{0} & \dots & (\boldsymbol{AB_{42}} \times \boldsymbol{B_{42}C_{12}}) \cdot \boldsymbol{W} \end{bmatrix} \quad (12)$$

The linear system becomes :

$$\begin{bmatrix} \boldsymbol{F_{ext}} & \boldsymbol{M_{ext}} & 0 & 0 \end{bmatrix}^t = J_b \begin{bmatrix} f_{11} & f_{12} & f_{21} & f_{22} & f_{31} & f_{32} & f_{41} & f_{42} \end{bmatrix}^t \quad (13)$$

Witch leads to:

$$\boldsymbol{F_b} = \mathbf{J_b^{-1}} \begin{bmatrix} \boldsymbol{F_{ext}} & \boldsymbol{M_{ext}} & 0 & 0 \end{bmatrix}^t \quad (14)$$

A plot of maximal forces in bars is presented in Fig 5b. For the selected geometry and dimensions, forces in bars are low and does not vary too much.

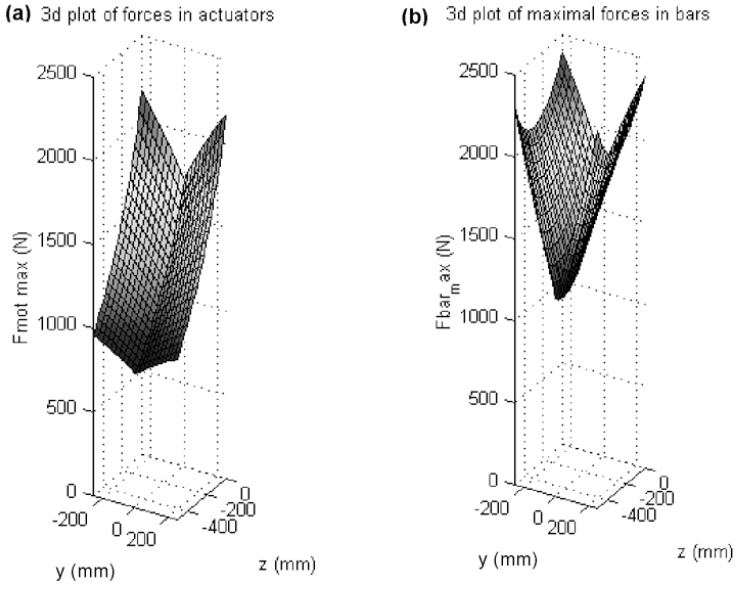

Fig. 5: *Maximal forces on the actuators and on the bars*

6 Stiffness analysis

It is obvious that for obtaining a good estimate of machine stiffness, a model using finite elements is needed. Nevertheless, such a model needs to know perfectly machine geometry and takes a lot of computing time. In a pre-sizing study it is better to have a simplified stiffness model taking only into account the less stiff parts. In this study, only stiffness of bars and stiffness of actuators are taken into account.

Given a force and torque on the nacelle, forces on actuators can be computed by equation (10). Assuming that :

– k_a is the actuator compliance along its direction of motion (all actuators are supposed to be identical)

– k_b is the compliance of a bar (all bars are supposed to be identical)

On one hand, displacement of actuators $\boldsymbol{dA} = [dA_1 \quad \dots \quad dA_4]^T$ can be written as follows (displacement of point A_i in direction of U_i):

$$\boldsymbol{dA} = \mathbf{M}\begin{bmatrix} \boldsymbol{F_{ext}} \\ \boldsymbol{M_{ext}} \cdot \boldsymbol{Z} \end{bmatrix} \tag{15}$$

with:

$$\mathbf{M} = k_a \, \mathbf{J}^{\mathbf{T}} \tag{16}$$

On the other hand, the displacement of points A_{ij} in direction of $\boldsymbol{U_i}$ is:

$$\mathbf{dA^*} = \mathbf{T_A}\left[\mathbf{F_{ext}} \quad \mathbf{M_{ext}} \quad 0 \quad 0\right] \tag{17}$$

with:

$$\begin{aligned} \boldsymbol{dA^*} &= [\boldsymbol{dA_{11}} \quad \boldsymbol{dA_{12}} \quad \dots \quad \boldsymbol{dA_{41}} \quad \boldsymbol{dA_{42}}]^T \\ \mathbf{TA} &= \mathbf{H_1 M H_2} \end{aligned} \tag{18}$$

and

$$\mathbf{H_1} = \begin{bmatrix} 1 & 1 & 0 & 0 & 0 & 0 & 0 & 0 \\ 0 & 0 & 1 & 1 & 0 & 0 & 0 & 0 \\ 0 & 0 & 0 & 0 & 1 & 1 & 0 & 0 \\ 0 & 0 & 0 & 0 & 0 & 0 & 1 & 1 \end{bmatrix} \text{ and } \mathbf{H_2} = \begin{bmatrix} 1 & 0 & 0 & 0 & 0 & 0 & 0 & 0 \\ 0 & 1 & 0 & 0 & 0 & 0 & 0 & 0 \\ 0 & 0 & 1 & 0 & 0 & 0 & 0 & 0 \\ 0 & 0 & 0 & 0 & 0 & 1 & 0 & 0 \end{bmatrix} \tag{19}$$

On the other hand, a change of bars length $\boldsymbol{dL}$ can be written as :

$$\boldsymbol{dL} = k_b \quad \boldsymbol{F_b} \tag{20}$$

$$\boldsymbol{dL} = k_b \quad \mathbf{J_b}^{-1} \begin{bmatrix} \boldsymbol{F_{ext}} \\ \boldsymbol{M_{ext}} \\ 0 \\ 0 \end{bmatrix} \tag{21}$$

The resulting displacement of the nacelle due to the change in bars length and actuator's position can be written by using the 8 following equations:

$$\boldsymbol{AB_{ij}} \cdot \boldsymbol{AB_{ij}} = L_{ij}{}^2 \tag{22}$$

This leads to :

$$\boldsymbol{AB_{ij}} \cdot \boldsymbol{AB_{ij}} = dL_{ij} \quad L_{ij} \tag{23}$$

Where :

– $\boldsymbol{dA_{ij}}$ is the displacement of point A_{ij}, due motors elasticity,

– $\boldsymbol{dB_{ij}}$ is the displacement of point B_{ij},

– dL_{ij} is the change in bars length due to deformation of bar number *ij*.

$\boldsymbol{dB_{ij}}$ can be easily found by the equations relative to small displacements:

$$\boldsymbol{dB_{ij}} = \begin{bmatrix} dx \\ dy \\ dz \end{bmatrix} + \boldsymbol{EB_{ij}} \times \begin{bmatrix} d\theta_x \\ d\theta_y \\ d\theta_z \end{bmatrix} + \boldsymbol{C_k B_{ij}} \times \left(d\omega_k \boldsymbol{W}\right) \tag{24}$$

Where:

– dx (namely dy, dz) is the displacement of point E about $\boldsymbol{x}$ axis (namely $\boldsymbol{y}$, z)

– $d\theta_x$ (namely $d\theta_y$, $d\theta_z$) is the rotation of the nacelle about $\boldsymbol{x}$ axis (namely $\boldsymbol{y}$, z)

– $d\omega_1$ (namely $d\omega_2$) is the rotation about $\boldsymbol{W}$ of $\boldsymbol{B_1B_2}$ ($\boldsymbol{B_3B_4}$)

– $k = 1$ *for* $i \in \{1, 2\}$, $k = 2$ *for* $i \in \{3, 4\}$

Assuming that:

$$\boldsymbol{dX} = \begin{bmatrix} dx & dy & dz & d\theta_x & d\theta_x & d\theta_x & d\omega_1 & d\omega_2 \end{bmatrix}^T \tag{25}$$

$$\boldsymbol{dB} = \begin{bmatrix} \boldsymbol{dB_{11}} \\ \boldsymbol{dB_{12}} \\ \dots \\ \boldsymbol{dB_{42}} \end{bmatrix} \text{ with } \boldsymbol{dB_{ij}} = \begin{bmatrix} dB_{ij,x} & dB_{ij,y} & dB_{ij,z} \end{bmatrix}^T \tag{26}$$

Equations (17) become:

$$\boldsymbol{dB} = \mathbf{M_X}\, \boldsymbol{dX} \tag{27}$$

Where:

$$\mathbf{M}\boldsymbol{X} = \begin{bmatrix} \mathbf{I}_3 & \mathbf{pre}(\boldsymbol{B_{11}E}) & \mathbf{pre}(\boldsymbol{B_{11}C_1}) & \mathbf{0} \\ \mathbf{I}_3 & \mathbf{pre}(\boldsymbol{B_{12}E}) & \mathbf{pre}(\boldsymbol{B_{12}C_1}) & \mathbf{0} \\ \dots & \dots & \dots & \dots \\ \mathbf{I}_3 & \mathbf{pre}(\boldsymbol{B_{41}E}) & \mathbf{0} & \mathbf{pre}(\boldsymbol{B_{41}C_2})\boldsymbol{W} \\ \mathbf{I}_3 & \mathbf{pre}(\boldsymbol{B_{42}E}) & \mathbf{0} & \mathbf{pre}(\boldsymbol{B_{42}C_2W}) \end{bmatrix} \tag{28}$$

Now, assuming that:

$$\mathbf{M_A} = \mathbf{diag}\left(\boldsymbol{AB_{ij}} \cdot \boldsymbol{U_i}\right) \tag{29}$$

$$\mathbf{M_B} = \begin{bmatrix} \boldsymbol{AB_{11}} & \boldsymbol{0} & \boldsymbol{0} & \boldsymbol{0} & \boldsymbol{0} & \boldsymbol{0} & \boldsymbol{0} & \boldsymbol{0} \\ \boldsymbol{0} & \boldsymbol{AB_{12}} & \boldsymbol{0} & \boldsymbol{0} & \boldsymbol{0} & \boldsymbol{0} & \boldsymbol{0} & \boldsymbol{0} \\ \boldsymbol{0} & \boldsymbol{0} & \boldsymbol{AB_{21}} & \boldsymbol{0} & \boldsymbol{0} & \boldsymbol{0} & \boldsymbol{0} & \boldsymbol{0} \\ \boldsymbol{0} & \boldsymbol{0} & \boldsymbol{0} & \boldsymbol{AB_{22}} & \boldsymbol{0} & \boldsymbol{0} & \boldsymbol{0} & \boldsymbol{0} \\ \boldsymbol{0} & \boldsymbol{0} & \boldsymbol{0} & \boldsymbol{0} & \boldsymbol{AB_{31}} & \boldsymbol{0} & \boldsymbol{0} & \boldsymbol{0} \\ \boldsymbol{0} & \boldsymbol{0} & \boldsymbol{0} & \boldsymbol{0} & \boldsymbol{0} & \boldsymbol{AB_{32}} & \boldsymbol{0} & \boldsymbol{0} \\ \boldsymbol{0} & \boldsymbol{0} & \boldsymbol{0} & \boldsymbol{0} & \boldsymbol{0} & \boldsymbol{0} & \boldsymbol{AB_{41}} & \boldsymbol{0} \\ \boldsymbol{0} & \boldsymbol{0} & \boldsymbol{0} & \boldsymbol{0} & \boldsymbol{0} & \boldsymbol{0} & \boldsymbol{0} & \boldsymbol{AB_{42}} \end{bmatrix} \tag{30}$$

$$\mathbf{M_L} = \mathbf{diag}\,(\boldsymbol{L}|_8) \tag{31}$$

Then equations (23) become:

$$\mathbf{M_B M_X}\, d\mathbf{X} = \mathbf{M_A}\, d\boldsymbol{A} + \mathbf{M_L}\, d\boldsymbol{L} \tag{32}$$

$$\mathbf{M_B M_X}\, d\boldsymbol{X} = (\mathbf{M_A T_A} + \mathbf{M_L T_L}) \boldsymbol{F_{ext}} \tag{33}$$

Finally:

$$d\boldsymbol{X} = (\mathbf{M_B M_X})^{-1} (\mathbf{M_A T_A} + \mathbf{M_L T_L}) \boldsymbol{F_{ext}} \tag{34}$$

That is to say:

$$d\boldsymbol{X} = \mathbf{K}\, \boldsymbol{F_{ext}} \tag{35}$$

Where the compliance matrix of the machine, **K**, is finally given by:

$$\mathbf{K} = (\mathbf{M_B M_X})^{-1} (\mathbf{M_A T_A} + \mathbf{M_L T_L}) \tag{36}$$

A plot of machine compliance is shown on Fig 6. Due to the machine geometry, the plot only concerns a (y, z) plane: the nacelle position along x axis does not influence the results. As expected from the results concerning maximal forces in actuators and bars, compliance decreases when the nacelle comes close to the actuators plane.

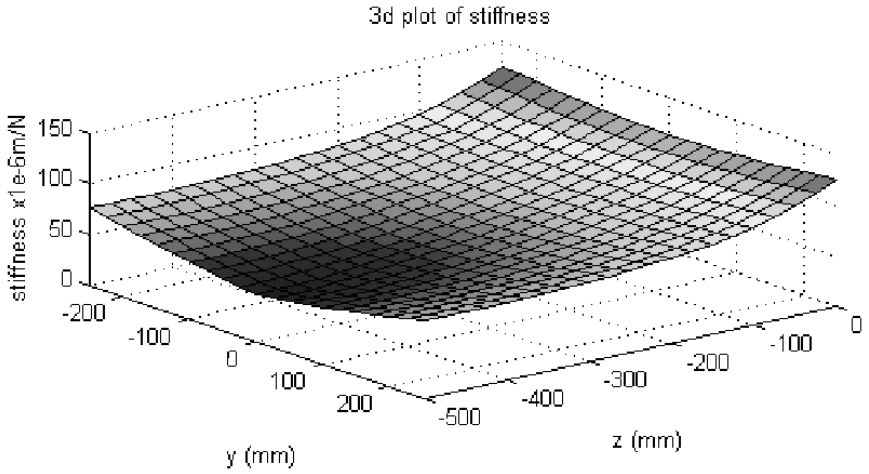

Fig. 6: *Stiffness plot*

8 Conclusion

In this case study, fast handling of heavy parts is considered as a potential application field for parallel mechanisms. A new machine concept is introduced to fulfil the key requirements of such an application. The mechanisms models are derived concerning geometry, workspace, kinematics, statics, stiffness and accuracy. A software module embedding all these tools have been written. The aim of this software is to offer a tool for obtaining preliminary results for the rough design and dimensioning of this family of four-degree-of-freedom parallel mechanisms. An appropriate interface let the user choose dimensional parameters of the machine for a given family of arrangements. Then some additional parameters are required as steps for computations, mass of parts, etc.

Plots of reachable workspace, well conditioned workspace, forces in actuators and bars, stiffness and accuracy are then available. It is obvious that, for the stiffness analysis, giving the simplified models used, the obtained results are less accurate than those provided by finite elements computations. This software represents the first step of the method for building the robot. It gives good estimates that help to make the choice for the machine elements. As many configurations as one wants can be checked because computation time is very short and changes in machine geometry can be easily done. On the other hand finite elements methods are more accurate but computation times are longer and it is more complicated to change the parameters of the machine, so this method must be used to refine the results given by the models presented in this paper.

The next steps of this research will be the definition of optimisation criterions and the construction of the real prototype based on the optimised mechanism.

Acknowledgements

This work has been partially supported by the European Commission (MACH21, GIRD CT1999 00150).

References

/1/ Company, O. Pierrot, F. Launay, F. and Fioroni, C. Modelling and preliminary design issues of a 3-axis parallel machine-tool. Proc. PKM-2000 conference, Ann Arbor, USA, 2000, 14-23.

/2/ Hesselbach, J. Plitea, N. Frindt, M. and Kusiek, A. A new parallel mechanism to use for cutting convex glass panels. In ARK, Strobl, 1998 165-174,

/3/ Koevermans, W.P. and al. Design and performance of the four d.o.f. motion system of the NLR research flight simulator. In AGARD Conf. Proc. No 198, Flight Simulation, La Haye, 1975, 17-1/17-11

/4/ Rolland, L.H. The Manta and the Kanuk novel 4-dof parallel mechanisms for industrial handling. In ASME Int. Mech. Eng. Congress, Nashville, 1999

/5/ Tanev, T.K. Forward displacement analysis of a three legged four-degree-of-freedom parallel manipulator. In ARK, Strobl, 1998, 147-154

/6/ Zlatanov, D. and Gosselin, C.M. A family of new parallel architectures with four degrees of freedom. In F.C. Park C.C. Iurascu, editor, Computational Kinematics, 2001, 57-66

/7/ Tsai, L-W. Kinematics of a three-dof platform with three extensible limbs. In J. Lenarcic V. Parenti-Castelli, editor, Recent Advances in Robot Kinematics, 401-410. Kluwer, 1996

/8/ Pierrot, F. and Company, O. H4: a new family of 4-degree of freedom parallel robots. AIM'99. Proc. IEEE/ASME International Conference on Advanced Intelligent Mechatronics, Atlanta, Georgia, USA, 1999, 508-513.

/9/ Yoshikawa, T. Manipulability of robotic mechanisms. In The International Journal of Robotics Research, vol 4-2, 1985 ,3-9

Appendix

Parameters for numerical examples (All dimensions are expressed in millimetres.)

$d = 100$ $p = 700$ $L = 1500$ $\boldsymbol{ED} = \begin{bmatrix} 0 & 0 & 300 \end{bmatrix}^T$ $\|\boldsymbol{B_{i1}}\ \boldsymbol{B_{i2}}\| = 100$

$$\mathbf{U} = \begin{bmatrix} -1 & 1 & 1 & -1 \\ 0 & 0 & 0 & 0 \\ 0 & 0 & 0 & 0 \end{bmatrix} \quad \boldsymbol{W} = \begin{bmatrix} 0 & 0 & 1 \end{bmatrix}^T \quad \mathbf{V} = \begin{bmatrix} 0.4615 & 0.4615 & 0.4615 & 0.4615 \\ 0.1925 & -0.1925 & 0.1925 & -0.1925 \\ 0.8660 & -0.8660 & -0.8660 & 0.8660 \end{bmatrix}$$

Maximal acceleration: ▶ for translation $\Gamma_{trans} = 5m / s^2$ ▶ for rotation $\Gamma_{rot} = 30rad / s^2$

$M_{nac} = 116kg$ inertia of the carried object $Iz = 0.38kgm^2$

Compliance ▶ of one bar $k_b = 1e^{-5}\ m/N$ ▶ of one actuator $k_a = 1e^{-4}$ m/N